Pyrazoles in Drug Discovery

Key Points

- May serve as a bioisostere to replace an arene or a hetarene with improved potency and physiochemical properties
- As a more lipophilic and more metabolically stable bioisostere for phenol

Overview

The pyrazole fragment may serve as a bioisostere to replace an arene or a hetarene with improved potency and physiochemical properties such as lipophilicity and aqueous solubility, etc. In addition, as an H-bond donating heterocycle, pyrazole has been employed as a more lipophilic and more metabolically stable bioisostere for phenol. Recent trend shows that more and more pyrazole-containing drugs are in drug pipelines.
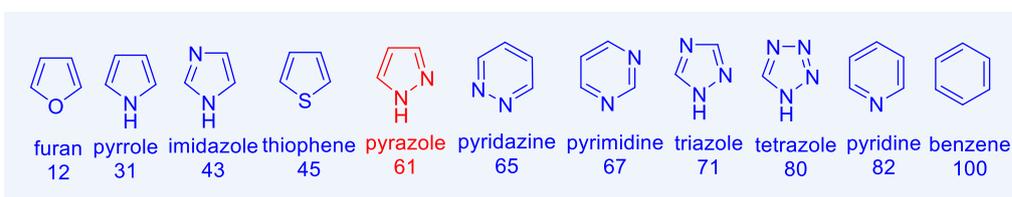
PharmaBlock

a = 1.349 Å
b = 1.331 Å
c = 1.416 Å
d = 1.373 Å
e = 1.359 Å

Pyrazole's Numbering and Bond Lengths

Pyrazole is a five-membered aromatic heterocycle with two N heteroatoms. Its N-1 is similar to the NH of pyrrole, and its N-2 behaves closely to the nitrogen atom of pyridine. Due to different bonding environments, all five bonds a–e have different bond lengths. Pyrazole's aromaticity lies somewhere in the middle of the scale among aromatic heterocycles:

furan 12 pyrrole 31 imidazole 43 thiophene 45 pyrazole 61 pyridazine 65 pyrimidine 67 triazole 71 tetrazole 80 pyridine 82 benzene 100

Relative Aromaticity of Aromatic Heterocycles

With a pKa of 2.5, pyrazole is significantly less basic than imidazole, whose pKa is 7.1. In fact, having an adjacent heteroatom near the N atom always has the effect of lowering the basicity of the N because of its inductive effect. Nonetheless, pyrazole is basic enough to be protonated with most strong inorganic acids. When pyrazole is unsymmetrically substituted, it may exist as a mixture of two tautomers. For instance, 5-methylpyrazole and 3-methylpyrazole coexist in a solution.
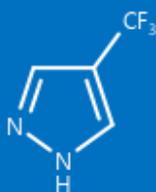

The ramification of the tautomerization is that alkylation of unsymmetrically substituted pyrazoles often gives rise to a mixture of two isomers, one is the *N*-1 alkylation and the other is the *N*-2 alkylation. The ratio depends on the nature of the substrate and the electrophile as well as on the solvent and base.
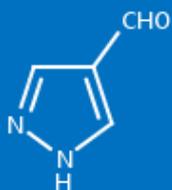
Pyrazole-containing Drugs

Not many pyrazoles exist in nature. However, over a dozen pyrazole-containing synthetic medicines are on the market. For instance, an anti-inflammatory cyclooxygenase-2 (COX-2) selective inhibitor celecoxib (Celebrex, **1**) has a tri-substituted pyrazole core structure.
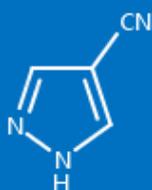
During the last few years, more and more pyrazole-containing drugs have gained regulatory approval, most conspicuously in the field of kinase inhibitors. Nearly all kinase inhibitors are competitive inhibitors, occupying the adenine triphosphate (ATP) binding pocket and replacing ATP. As a consequence, all of the ATP-competitive kinase inhibitors possess a flat aromatic core structure, mimicking the adenine portion of ATP. Thanks to pyrazole's aromaticity, it is making frequent appearances in the realm of kinase inhibitors. Pfizer's first-in-class dual anaplastic lymphoma kinase (ALK) and mesenchymal−epithelial transition factor (c-MET) inhibitor, crizotinib (Xalkori, **2**), contains a di-substituted pyrazole. It was discovered using sunitinib-like 3-substituted indolin-2-ones as the starting point. The co-crystal structure of crizotinib (**2**) and the c-MET protein indicated that the 5-pyrazol-4-yl group is bound through the narrow lipophilic tunnel surrounded by Ile-1084 and Tyr-1159.[1] Since crizotinib (**2**) has little CNS exposure, Pfizer, guided by structure-based drug design (SBDD), lipophilicity efficiency (LipE), and physical property-based optimization, converted the crizotinib (**2**) to macrocycles. Among them, lorlatinib (Lorbrena, **3**) emerged with good absorption, distribution, metabolism, and excretion (ADME), low propensity for p-glycoprotein (pgp) 1-mediated efflux, and good passive permeability with significant CNS exposure. It is thus suitable for treating metastasized brain tumors.[2]

Janus kinases (JAK) recruit signal transducers and activators of transcription (STATS) to cytokine receptors, leading to modulation of gene expression. Incyte was one of the pioneers in the discovery of JAK inhibitors. Their pyrazole-containing ATP-competitive JAK1/2 dual inhibitor ruxolitinib (Jakafi, **4**) was approved by the FDA in 2011 for the treatment of patients with myelofibrosis (MF, a bone marrow disorder). Incyte's *encore* JAK1/2 dual inhibitor baricitinib (Olumiant, **5**) was marketed in 2017 for treating rheumatoid arthritis (RA).
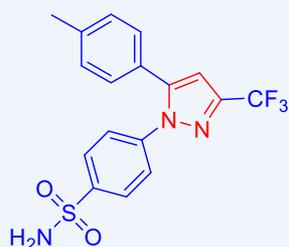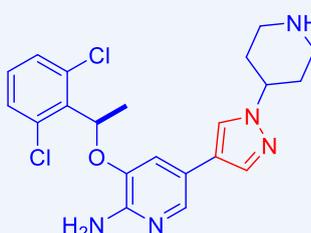
PharmaBlock Products

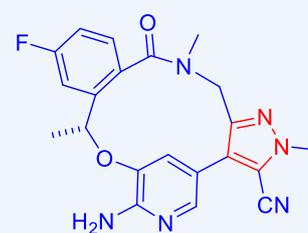**PB113097**

PBN2011211

Approximately ten dipeptidyl peptidase-4 (DPP4) inhibitors are currently available for the treatment of type II diabetes mellitus (T2DM). One of them, Mitsubishi's teneligliptin (Tenelia, **6**), has a tri-substituted pyrazole core structure. Lexicon's tryptophan hydroxylase inhibitor telotristat ethyl (Xermelo, **7**) was approved in 2017. In 2018, Array/Novartis' B-raf kinase inhibitor, encorafenib (Braftovi, **8**), gained the nod from the FDA for treating melanoma and colorectal cancers. It is a tri-substituted pyrazole.
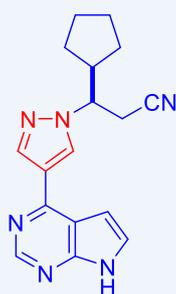

celecoxib (Celebrex, **1**)
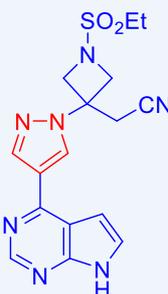Pfizer, 1998
COX-2 inhibitor

crizotinib (Xalkori, **2**)
Pfizer, 2011
ALK inhibitor

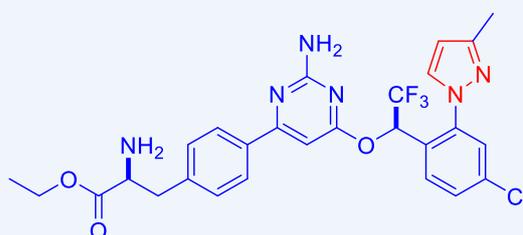lorlatinib (Lorbrena, **3**)
Pfizer, 2018
ALK inhibitor

ruxolitinib (Jakafi, **4**)
Incyte, 2010
JAK1/2 inhibitor

baricitinib (Olumiant, **5**)
Incyte/Lilly, 2017 (for RA)
JAK1/2 inhibitor

teneligliptin (Tenelia, **6**)
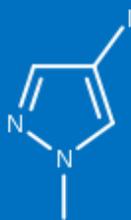Mitsubishi Tanabe, 2012 (Japan)
DPP-4 inhibitor

telotristat ethyl (Xermelo, **7**)
Lexicon, 2017
tryptophan hydroxylase inhibitor

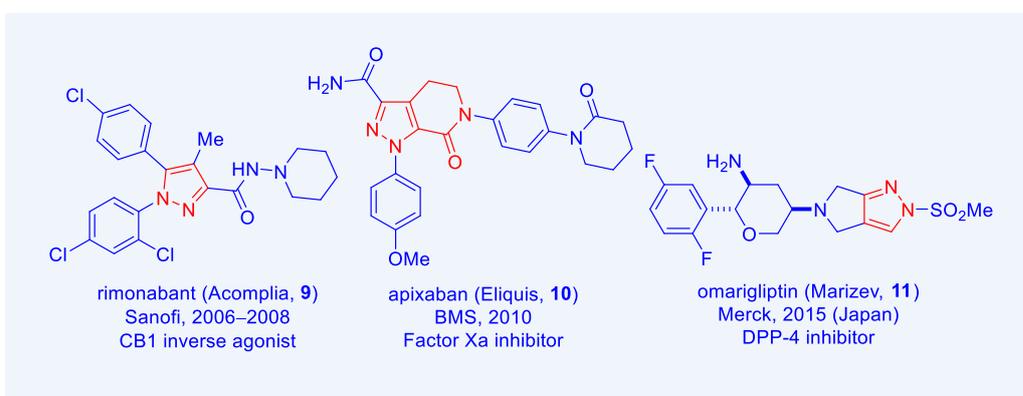encorafenib (Braftovi, **8**)
Novartis, 2018
B-raf inhibitor

A fully substituted pyrazole, rimonabant (Acomplia, **9**), is a selective inverse agonist for the cannabinoid receptor type 1 (CB$_1$). It was marketed in 56 countries for the treatment of obesity by Sanofi−Aventis starting in 2006, but was withdrawn in 2008 due to an unfavorable benefit/toxicity profile including the risk of serious psychiatric problems.
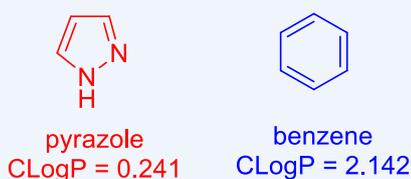
Several pyrazole-fused drugs are also on the market. In addition to the well-known phosphodiesterase V (PDE5) inhibitor sildenafil (Viagra), they also include BMS's factor Xa inhibitor apixaban (Eliquis, **10**) and Merck's DPP-4 inhibitor omarigliptin (Marizev, **11**).
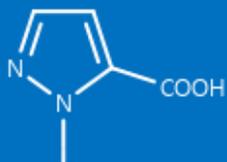

rimonabant (Acomplia, **9**)
Sanofi, 2006−2008
CB1 inverse agonist

apixaban (Eliquis, **10**)
BMS, 2010
Factor Xa inhibitor

omarigliptin (Marizev, **11**)
Merck, 2015 (Japan)
DPP-4 inhibitor

Pyrazoles in Drug Discovery

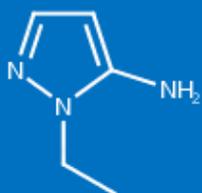**a.   Pyrazole as a bioisostere of arenes and hetarenes**

With regard to aromaticity, pyrazole (65%) is not the closest to that of benzene's (100%). However, the former is significantly less lipophilic (CLogP = 0.241) than the latter (CLogP = 2.142). Therefore, pyrazole has been employed as a bioisostere for benzene and other arenes, resulting in improved potency and physiochemical properties, such as lipophilicity and aqueous solubility, etc.
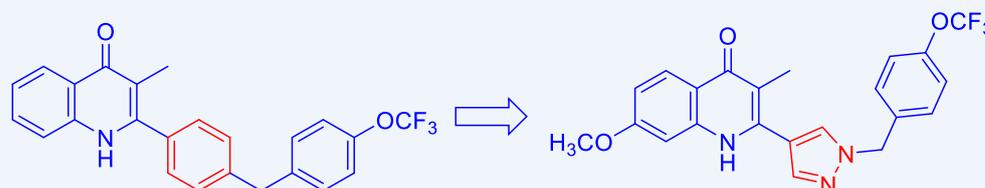

pyrazole
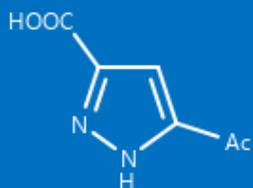CLogP = 0.241

benzene
CLogP = 2.142

While 2-aryl quinolone **12** demonstrated good antimalarial activities against various strains of *P. falciparum* by inhibiting two mitochondrial enzymes in the electron transport chain, the cytochrome bc_1 complex and type-II NADH:ubiquinone oxidoreductase (PfNDH2), its physiochemical properties needed optimization. Replacing the central phenyl ring with a pyrazole group resulted in a series of 2-pyrazolyl quinolones with improved antimalarial potency and various *in vitro* drug metabolism and pharmacokinetics (DMPK) features. In particular, 2-pyrazolyl quinolone **13** displayed no cross-resistance with multidrug resistant parasite strains (W2) compared to drug sensitive strains (3D7), with IC_{50} values in the range of 15–33 nM. Furthermore, 2-pyrazolyl quinolone **13** also retained moderate activity against the atovaquone-resistant parasite isolate (TM90C2B). It also displayed improved DMPK properties, including improved aqueous solubility compared to previously reported quinolone series as represented by 2-aryl quinolone **12**, as well as acceptable safety margin through *in vitro* cytotoxicity assessment.[3]
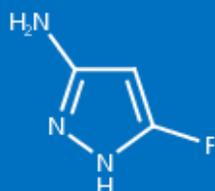

2-aryl quinolone **12**
IC_{50} (3D7) = 117 nM
IC_{50} (W2) = 26 nM
IC_{50} (TM90C2B) = 122 nM
aq. sol. (pH7.4) = 0.03 μM
cLogP = 5.67

2-pyrazolyl quinolone **13**
IC_{50} (3D7) = 33 nM
IC_{50} (W2) = 15 nM
IC_{50} (TM90C2B) = 500 nM
aq. sol. (pH7.4) = 0.3 μM
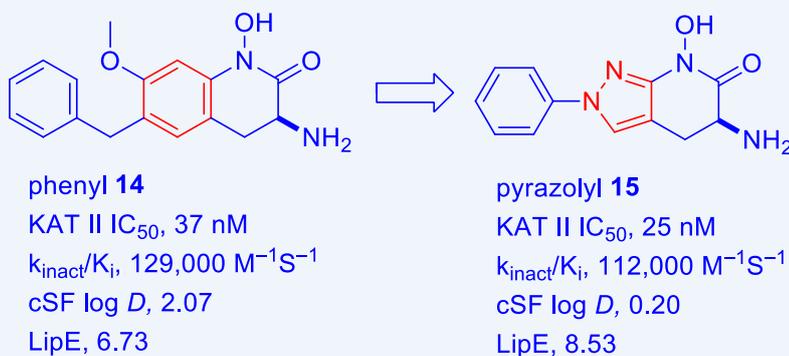cLogP = 3.70
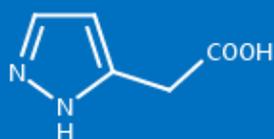TI = 333

PharmaBlock Products

PBZ1588

PB201304002

Inhibition of kynurenine aminotransferase (KAT) II may offer a new therapeutic approach for schizophrenia and other CNS diseases. Pfizer's irreversible KAT II inhibitor **14** was found to be very potent, forming a covalent bond with the enzyme's cofactor pyridoxal phosphate (PLP) in the enzyme active site. In order to reduce phenyl **14**'s lipophilicity, Dounay and colleagues chose pyrazole as a replacement of the phenyl core structure, arriving at a new series of pyrazoles that possessed superior physiochemical properties. A representative, pyrazolyl **15**, had a 10-fold drop of calculated shake flask (cSF) distribution coefficient (log D) at pH7.4 in comparison to **14**. Its lipophilic efficiency (LipE) was 8.53, a nearly 2-log boost from its prototype **14**.[4]

phenyl **14**
KAT II IC_{50}, 37 nM
k_{inact}/K_i, 129,000 $M^{-1}S^{-1}$
cSF log D, 2.07
LipE, 6.73

pyrazolyl **15**
KAT II IC_{50}, 25 nM
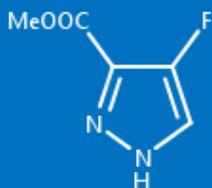k_{inact}/K_i, 112,000 $M^{-1}S^{-1}$
cSF log D, 0.20
LipE, 8.53

Du Pont's losartan (Cozarr, **16**) was the first selective non-peptide angiotensin II receptor antagonist on the market for treating hypertension. It was soon discovered that its carboxylic acid metabolite, imidazole acid **17**, was significantly more potent than losartan (**16**) with similar or longer duration of action. Merck initially explored triazole analogues in place of losartan (**16**)'s imidazole, but triazoles were generically covered by Du Pont's patent application. To circumvent the intellectual property (IP) issue, Merck switched to pyrazole as the bioisostere of losartan's imidazole moiety. To that end, they discovered a series of pyrazole compounds as represented by pyrazole **18**, which had similar potency as the imidazole derivatives.[5]
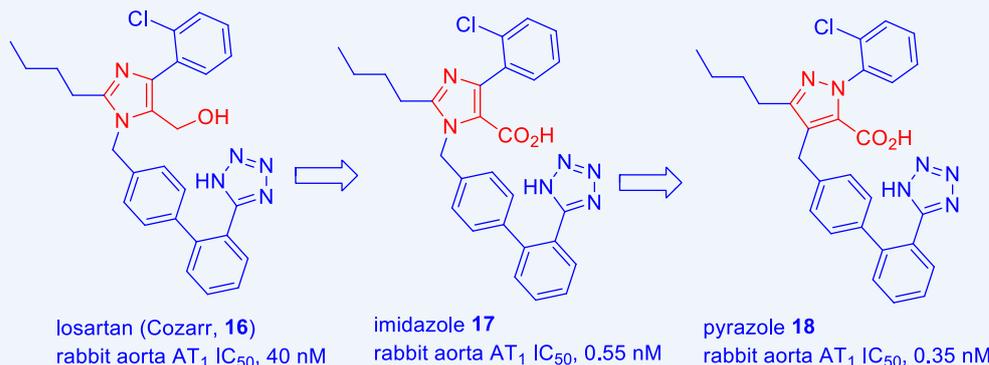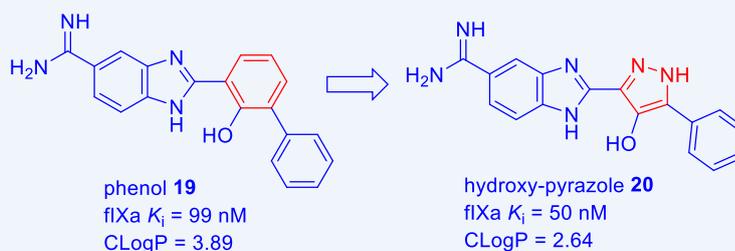
PharmaBlock Products

PB07688

PBXA1250

losartan (Cozarr, **16**)
rabbit aorta AT_1 IC_{50}, 40 nM

imidazole **17**
rabbit aorta AT_1 IC_{50}, 0.55 nM
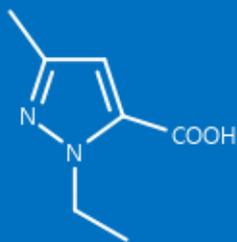
pyrazole **18**
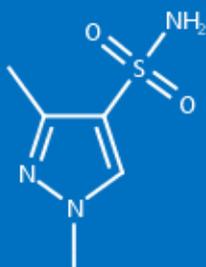rabbit aorta AT_1 IC_{50}, 0.35 nM

The enormous success of apixaban (Eliquis, **10**) proved that factor Xa inhibition is a valid approach for discovering anticoagulants. Factor IXa inhibitors, in the same vein, have also shown promises in modulating the intrinsic pathway of the blood clotting cascade. Celera initially obtained phenol **19** with an IC_{50} value of 99 nM for factor IXa as a reasonable lead. However, the potency was not translated into observed efficacy in *ex vivo* clotting efficacy assays, possibly because of **19**'s unfavorable physiochemical properties. Replacing phenol with hydroxypyrazole as a bioisostere led to compound **20**, which showed similar potency without significantly increasing the molecular weight. Furthermore, the more polar pyrazole analogue **20** had improved physiochemical properties, which translated into better *ex vivo*

phenol **19**
fIXa K_i = 99 nM
CLogP = 3.89

hydroxy-pyrazole **20**
fIXa K_i = 50 nM
CLogP = 2.64
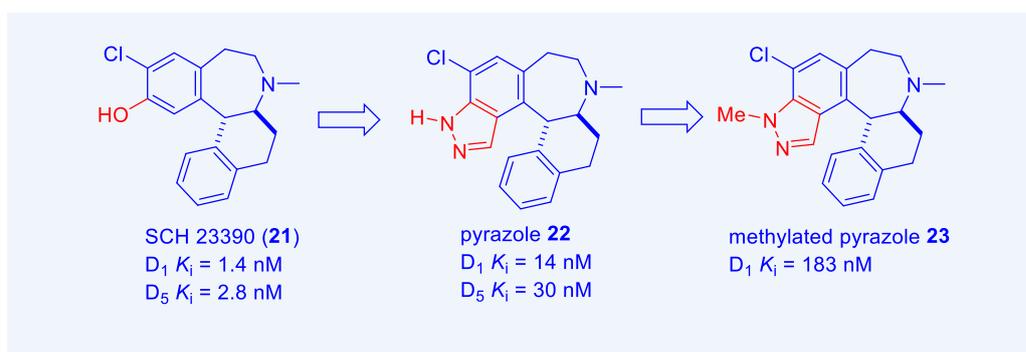
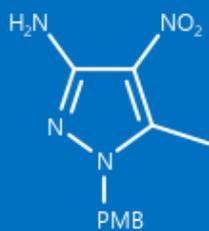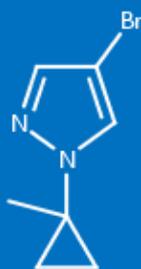## b. Pyrazole as hydrogen bond donor and acceptor

Back in the 1980s, Schering−Plough reported the discovery of the first high-affinity and selective D_1/D_5 antagonist SCH 23390 (**21**). However, benzazepine **21** was inactive in rhesus monkeys with a very short duration of action. Pharmacokinetic evaluation revealed that extensive *O*-glucuronidation of the phenol and *N*-dealkylation of the N-Me group *in vivo* may contributed to the poor PK profile. Taking a page from Lilly's[7a] and Purdue's[7b] exploits of pyrazole bioisostere for phenol in the dopaminergic field, Schering−Plough chose to replace the metabolically problematic phenol with pyrazole and other heterocycles with hydrogen bond donating NH functionality. Generally speaking, phenol's heterocyclic bioisosteres tend to be more lipophilic and less vulnerable to phase I and II metabolism in comparison to phenol. Indazole **22** was tested about ten-fold less potent than SCH 23390 (**21**) but began to show improved PK profile. As a testimony to the importance of the hydrogen bond donating NH functionality, methylated indazole **23** had significantly decreased affinity for the D_1 receptor.[7c]

SCH 23390 (**21**)
D_1 K_i = 1.4 nM
D_5 K_i = 2.8 nM

pyrazole **22**
D_1 K_i = 14 nM
D_5 K_i = 30 nM

methylated pyrazole **23**
D_1 K_i = 183 nM
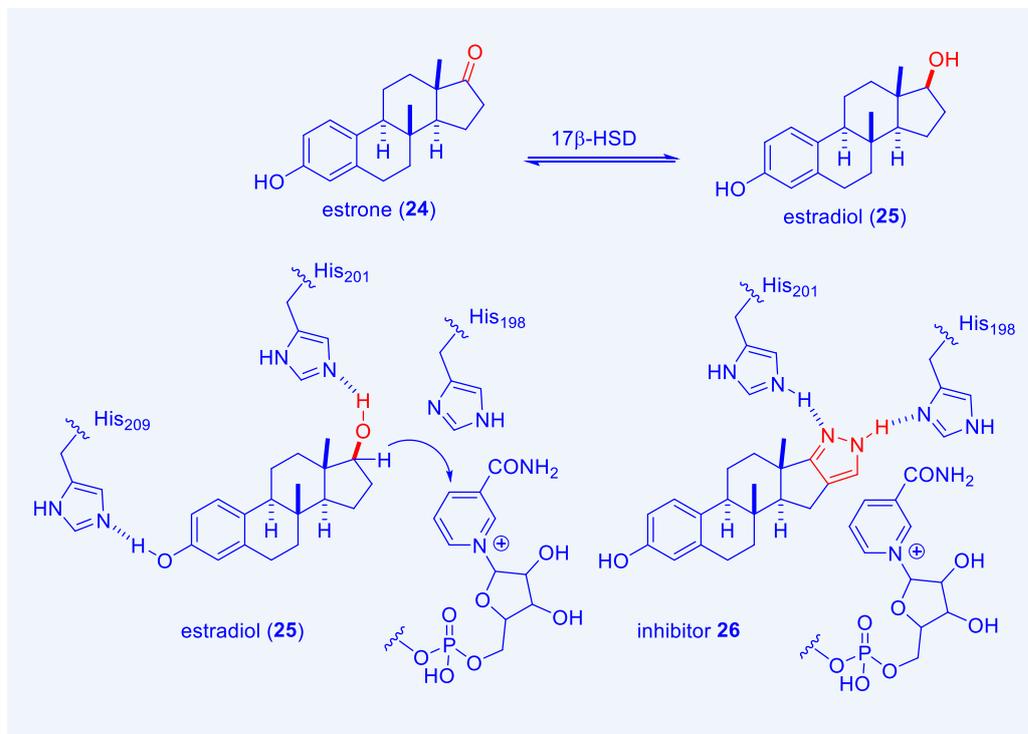
PharmaBlock Products

PBHM9137

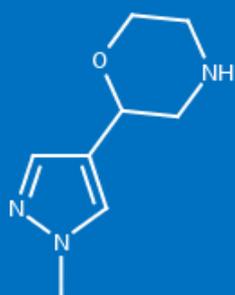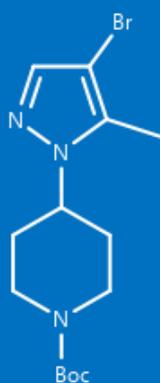**PBHMA108**

17β-Hydroxysteroid dehydrogenase (17β-HSD) catalyzes the reduction of estrone (**24**) to estradiol (**25**). 17β-HSD inhibitors have shown promises in several therapeutic areas including oncology, CNS, and osteoporosis. It was speculated that hydrogen bonds between estone (**24**) [or estradiol (**25**)] and the catalytically active His_{198} and His_{201} of the 17β-HSD protein stabilize substrate complexes as shown on the bottom left in the figure below. This hypothesis was supported by the affinity shown by the pyrazole analogue **26**. While estrone (**24**) had a K_i value of 9.50 µM, inhibitor **26** had a K_i value of 4.08 µM, heterocycle such as isoxazole without a hydrogen bond donor was significantly less active. For pyrazole **26**, its NH donating an H-bond to His_{198}, with His_{201} adopting a tautomeric configuration in order to donate an H-bond to the pyrazole nitrogen atom as depicted by the structure at the bottom right corner in the figure shown below. The potency difference between estrone (**24**) and inhibitor **26** was attributed to an additional H-bond donor interaction to His_{198} by the pyrazole NH.[8]
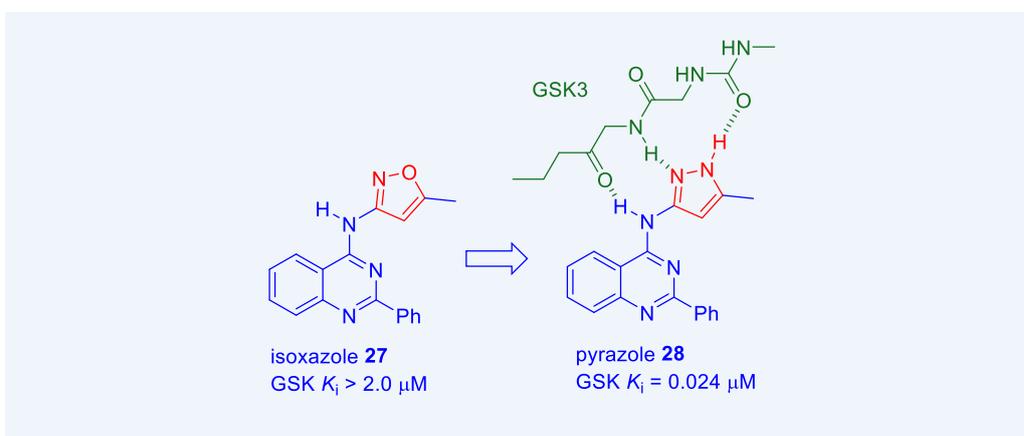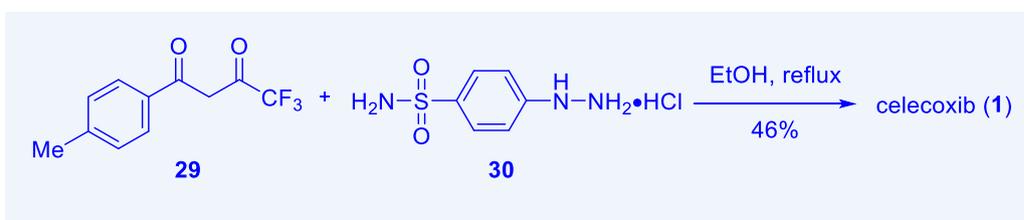
The serine/threonine kinase glycogen synthase kinase 3 (GSK3) inhibitors have been investigated as potential therapies for T2DM and Alzheimer's disease (AD). Vertex's quinazoline series GSK3 inhibitors highlighted the importance of H-bonds in kinase ligand design. Although the isoxazole analogue **27** was virtually inactive, pyrazole **28** was potent and exhibited inhibition kinetics consistent with the compound acting as a competitive inhibitor of ATP binding. An X-ray co-crystal structure confirmed the mode of inhibition and revealed three H-bonding interactions between the GSK3 enzyme and pyrazole **28**, which adopted an overall *planar* topography in the active site, as shown below.[9]
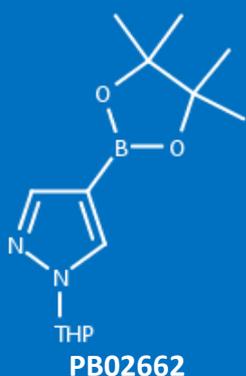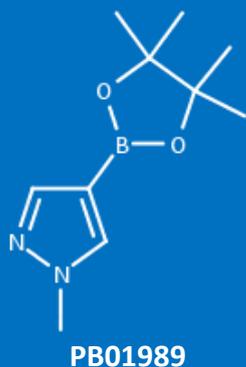

isoxazole **27**
GSK K_i > 2.0 μM

pyrazole **28**
GSK K_i = 0.024 μM
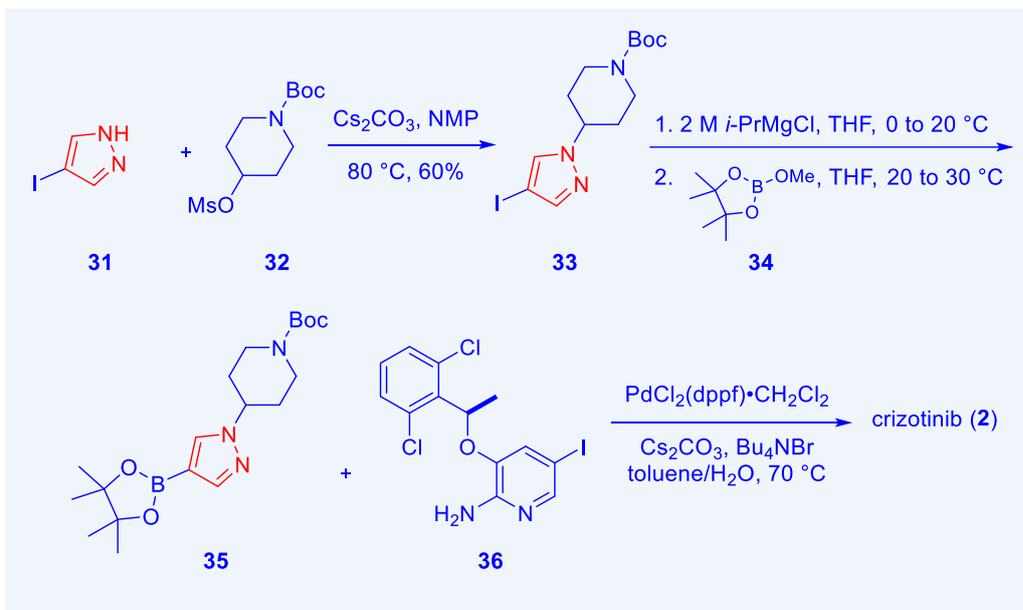
Synthesis of Some Pyrazole-containing Drugs

Production of celecoxib (**1**) is very straightforward. It entails simple condensation between dione **29** and 4-sulfonamidophenylhydrazine hydrochloride (**30**) to deliver the desired diarylpyrazole **1**.[10]
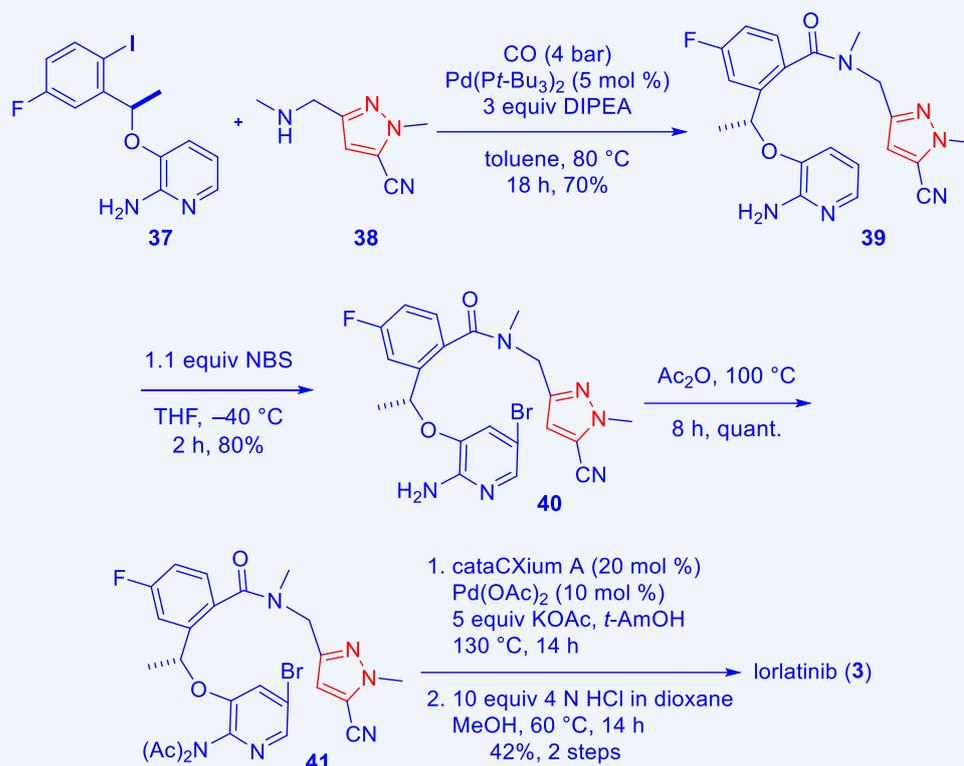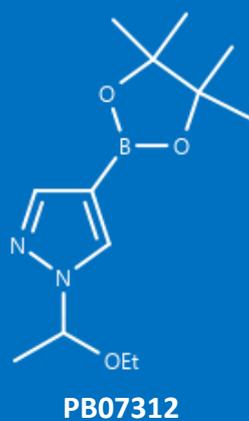
PharmaBlock Products
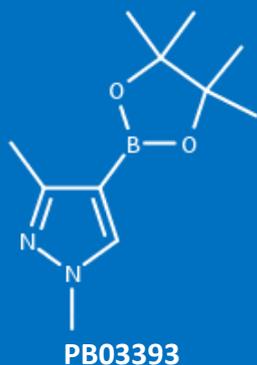

PB01989

PB02662

Pfizer's synthesis of its ALK inhibitor crizotinib (**2**) began with an S_N2 reaction between 4-iodo-1*H*-pyrazole (**31**) and mesylate **32**. The resulting adduct **33** underwent a halogen–metal exchange, followed by quenching with borolane reagent **34** to afford arylboronate **35**. Finally, a Suzuki coupling with between **35** and iodide **36** delivered crizotinib (**2**).[1]
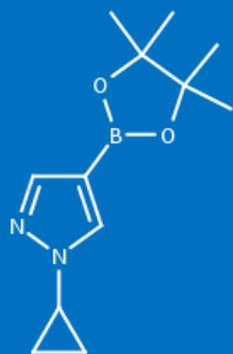

For the preparation of Pfizer's macrocyclic ALK inhibitor lorlatinib (**3**), a palladium-catalyzed aminocarbonylation between aryl iodide **37** and pyrazole amine **38** assembled the linear precursor **39**. After regioselective bromination of **39** with NBS, the resulting bromide **40** was protected as its bis-acetamide **41** otherwise the palladium-catalyzed cyclization did not work. Eventually, an intramolecular arylation of **41** was followed by de-protection to offer lorlatinib (**3**).[2]

PharmaBlock Products
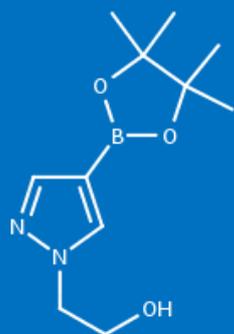

PB03393

PB07312

Incyte's synthesis of their JAK1/2 inhibitor ruxolitinib (**4**) commenced with a Suzuki coupling between chloropyrrolopyrimidine **42** and pyrazole pinacolatoboronate **43** to assemble pyrazole **44**. *aza*-Michael addition of pyrazole **44** to 3-cyclopentylacrylonitrile (**45**) was promoted by DBU to arrive at SEM-protected ruxolitinib **46** in excellent yield. Chiral separation of the two resultant enantiomers was followed by deprotection, salt formation, and recrystallization to produce ruxolitinib (**4**).[11]
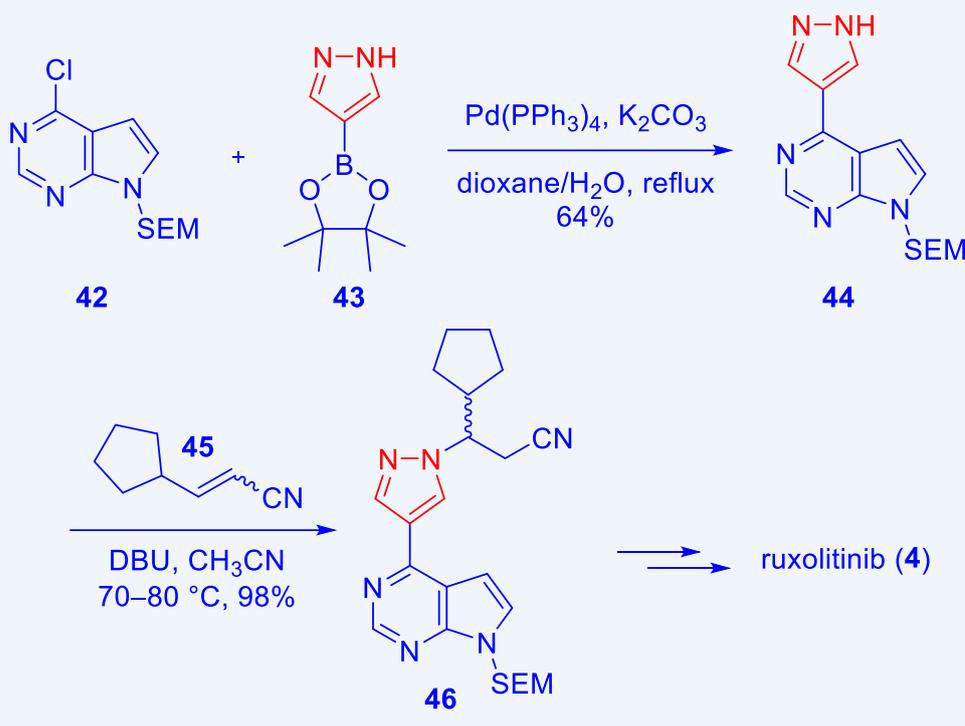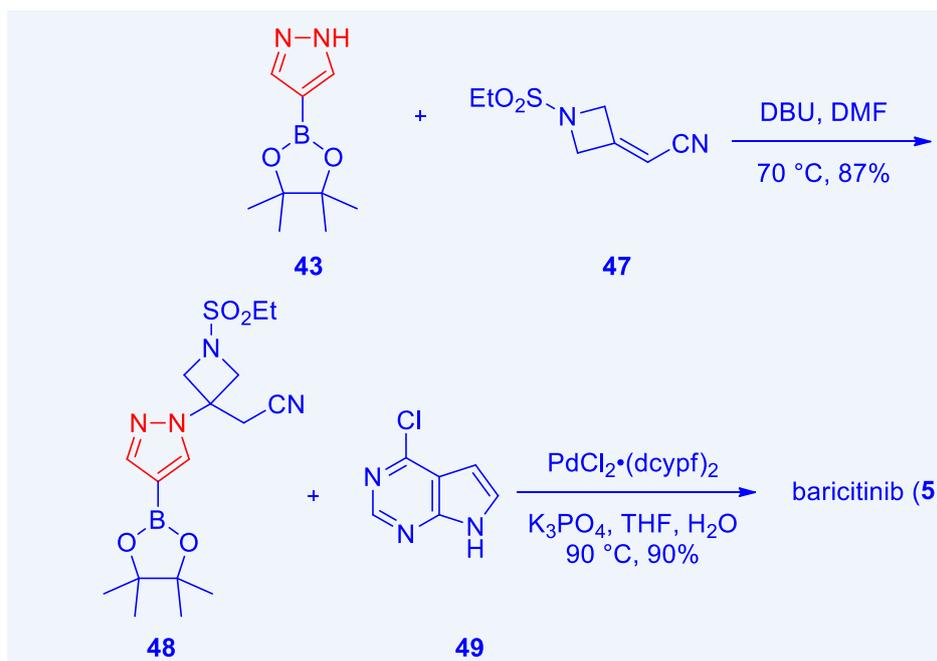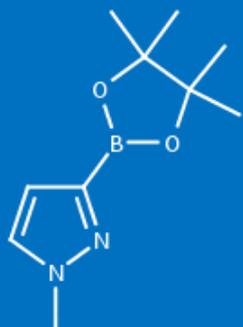
PharmaBlock Products
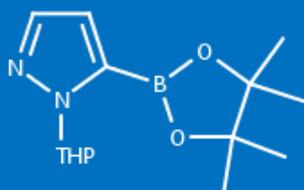

PB06600

PBN20121663

The aforementioned tactic of *aza*-Michael addition of pyrazole to an acrylonitrile was also employed in one of the syntheses of Incyte's second JAK1/2 inhibitor baricitinib (**5**). To that end, *aza*-Michael addition of the same pyrazole **43** to cyanomethylazetidine **47** gave rise to pinacolatoboronate **48**. The final Suzuki coupling between **48** and chloropyrrolopyrimidine **49** proceeded smoothly *without* protection of the pyrrole NH to deliver baricitinib (**5**).[12]
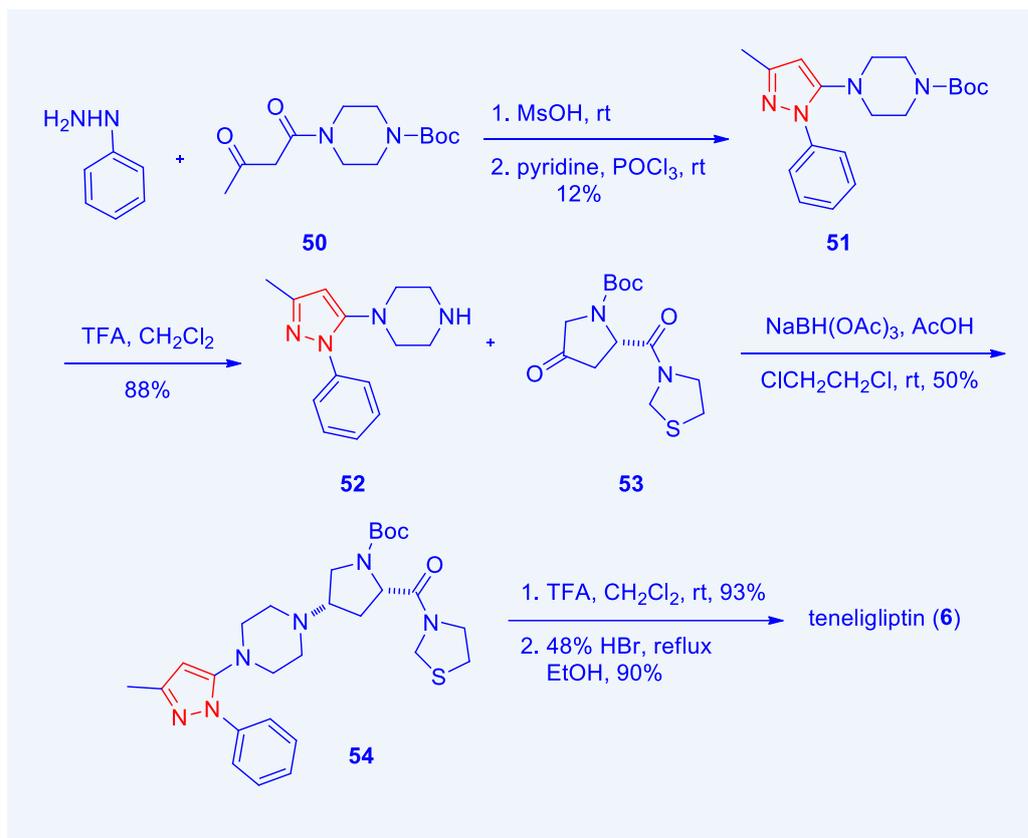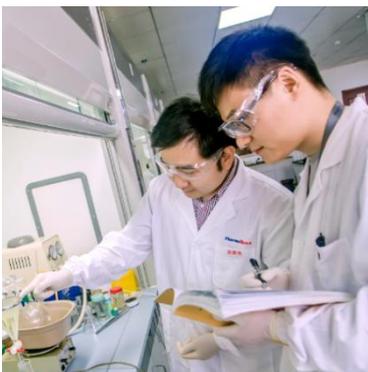
PharmaBlock Products

PBSQ8184

PB02569

The only reported synthetic approach of DPP4 inhibitor teneligliptin (**6**) began with condensation of phenylhydrazine with acetoacetamide **50**, followed by cyclodehydration, to produce pyrazole **51**. After removal of the Boc protection, the resultant piperazine **52** underwent a reductive amination with amide-ketone **53** to assemble adduct **54**. Deprotection of the second Boc group and HBr salt formation then give rise to teneligliptin (**6**).[13]
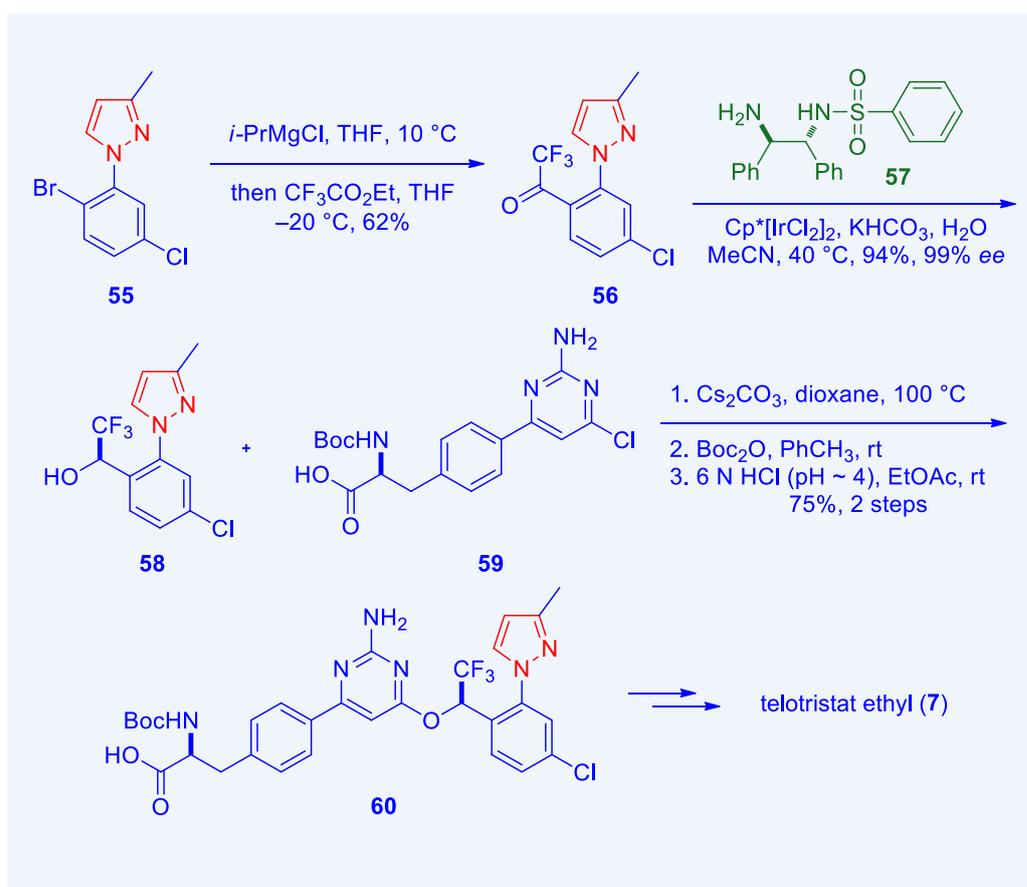
Preparation of the pyrazole fragment on Lexicon's tryptophan hydroxylase inhibitor telotristat ethyl (**7**) involves an interesting asymmetric reduction of a ketone. Thus, the halogen–metal exchange intermediate from bromide **55** was quenched by ethyl trifluoroacetate to afford ketone **56**. Asymmetric reduction of **56** was accomplished via an iridium-catalyzed hydride transfer with the aid of a chiral ligand **57** to give trifluoroalcohol **58** without resorting to any silica gel chromatography thus far. Subsequently, an S$_N$Ar reaction between **58** and pyrimidylchloride **59** gave rise to adduct **60**. Since the reaction conditions were harsh enough to partially remove the Boc protection, it was put back on to help purification. Adjustment of the reaction to pH ~ 4 using 6 N HCl was key to ensure a good overall yield. After purification, Boc protective group was removed and the ethyl ester was installed to provide telotristat ethyl (**7**). The API was then prepared as the hippurate salt.[14]

Novartis's synthesis of the B-raf inhibitor encorafenib (**8**) resorted conversion of pyrazole-amine **61** to the corresponding iodide **62** via the intermediacy of its diazonium salt. A two-step sequence involving *N,N*-dimethyformamide dimethyl acetal (DMF-DMA) and guanidine hydrochloride constructed the aminopyrimidine **63**. The amine functionality was converted to the alcohol, which was subsequently chlorinated to offer chloropyrimidine **64**. An S$_N$Ar reaction between **64** and primary amine **65** assembled **66**, which underwent a Suzuki coupling with pinacolatoboronate **67** to deliver encorafenib (**8**).[15]

In summary, the pyrazole fragment may serve as a bioisostere to replace an arene or a hetarene with improved potency and physiochemical properties, such as lipophilicity and aqueous solubility, etc. In addition, as an H-bond donating heterocycle, pyrazole has been employed as a more lipophilic and more metabolically stable bioisostere for phenol. Recent trend shows that more and more pyrazole-containing drugs are in drug pipelines.

References

1. Cui, J. J.; Tran-Dube, M.; Shen, H.; Nambu, M.; Kung, P.-P.; Pairish, M.; Jia, L.; Meng, J.; Funk, L.; Botrous, I.; et al. *J. Med. Chem.* **2011,** *54*, 6342–6363.

2. Johnson, T. W.; Richardson, P. F.; Bailey, S.; Brooun, A.; Burke, B. J.; Collins, M. R.; Cui, J. J.; Deal, J. G.; Deng, Y.-L.; Dinh, D.; et al. *J. Med. Chem.* **2014,** *57*, 4720–4744.

3. Hong, W. D.; Leung, S. C.; Amporndanai, K.; Davies, J.; Priestley, R. S.; Nixon, G. L.; Berry, N. G.; Hasnain, S. S.; Antonyuk, S.; Ward, S. A.; et al. *ACS Med. Chem. Lett.* **2018,** *9*, 1205–1210.

4. Dounay, A. B.; Anderson, M.; Bechle, B. M.; Evrard, E.; Gan, X.; Kim, J.-Y.; McAllister, L. A.; Pandit, J.; Rong, S. B.; Salafia, M. A.; et al. *Bioorg. Med. Chem. Lett.* **2013,** *23*, 1961–1966.

5. Ashton, W. T.; Hutchins, S. M.; Greenlee, W. J.; Doss, G. A.; Chang, R. S. L.; Lotti, V. J.; Faust, K. A.; Chen, T. B.; Zingaro, G. J.; et al. *J. Med. Chem.* **1993,** *36*, 3595–3605.

6. Vijaykumar, D.; Sprengeler, P. A.; Shaghafi, M.; Spencer, J. R.; Katz, B. A.; Yu, C.; Rai, R.; Young, W. B.; Schultz, B.; Janc, J. *Bioorg. Med. Chem. Lett.* **2006,** *16*, 2796–2799.

7. (a) Bach, N. J.; Kornfeld, E. C.; Clemens, J. A.; Smalstig, E. B. *J. Med. Chem.* **1980,** *48*, 812–814. (b) Doll, M. K.-H.; Nichols, D. E.; Kilts, J. D.; Prioleau, C.; Lawler, C. P.; Lewis, M. M.; Mailman, R. B. *J. Med. Chem.* **1999,** *42*, 935–940. (c) Wu, W.-L.; Burnett, D. A.; Spring, R.; Greenlee, W. J.; Smith, M.; Favreau, L.; Fawzi, A.; Zhang, H.; Lachowicz, J. E. *J. Med. Chem.* **2005,** *48*, 680–693.

8. Sweet, F.; Boyd, J.; Medina, O.; Konderski, L.; Murdock, G. L. *Biochem. Biophys. Res. Commun.* **1991,** *180*, 1057–1063.

9. Pierce, A. C.; ter Haar, E.; Binch, H. M.; Kay, D. P.; Patel, S. R.; Li, P. *J. Med. Chem.* **2005,** *48*, 1278–1281.

10. Penning, T. D.; Talley, J. J.; Bertenshaw, S. R.; Carter, J. S.; Collins, P. W.; Docter, S.; Graneto, M. J.; Lee, L. F.; Malecha, J. W.; Miyahiro, J. M.; et al. *J. Med. Chem.* **1997,** *40*, 1347–1365.

11. Zhou, J.; Liu, P.; Lin, Q.; Metcalf, B. W.; Meloni, D.; Pan, Y.; Xia, M.; Li, M.; Yue, T.-Y.; Rodgers, J. D.; Wang, H. WO 2010083283 A2 (2010).

12. Xu, J.; Cai, J.; Chen, J.; Zong, X.; Wu, X.; Ji, M.; Wang, P. *J. Chem. Res.* **2016,** *40*, 205–208.

13. Yoshida, T.; Akahoshi, F.; Sakashita, H.; Kitajima, H.; Nakamura, M.; Sonda, S; Takeuchi, M.; Tanaka, Y.; Ueda, N.; Sekiguchi, S.; et al. *Bioorg. Med. Chem.* **2012,** *20*, 5705–5719.

14. (a) Bednarz, M. S.; Burgoon, H. A., Jr.; Iimura, S.; Kanamarlapudi, R. C.; Song, Q.; Wu, W.; Yan, J.; Zhang, H. WO 2009029499A1 (2009). (b) Bednarz, M. S.; De Paul, S.; Kanamarlapudi, R. C.; Perlberg, A.; Zhang, H. WO 2009042733A1 (2009).

15. Huang, S.; Jin, X.; Liu, Z.; Poon, D.; Tellew, J.; Wan, Y.; Wang, X.; Xie, Y. WO 2011025927 (2011).